

Experimental and thermodynamic analysis of a compression ignition engine operating with straight soybean oil

Nury A. Nieto Garzón · Amir A. M. Oliveira ·
Ricardo Morel Hartmann · Edson Bazzo

Received: 17 April 2014 / Accepted: 25 November 2014 / Published online: 13 December 2014
© The Brazilian Society of Mechanical Sciences and Engineering 2014

Abstract This paper presents an experimental and thermodynamic analysis of a compression ignition engine with rated power of 14.7 kW, fueled with diesel oil, straight soybean oil, and blend of 50 % (v/v) soybean and diesel oils. The experimental work consisted in characterization of physical–chemical properties of the fuels and steady-state measurements of brake power, fuel consumption and exhaust gas emissions (CO, CO₂ and NO_x) as function of engine speed. Thermodynamic analysis was carried out at 1,800 rpm. The results were evaluated applying analysis of variance and the Dunnett's test. The engine operation with soybean oil in comparison with diesel oil showed reduction in power, increase in fuel consumption, similar fuel conversion efficiency, exergetic efficiency and exergy destruction. Analysis at 1,800 rpm for operation with soybean oil revealed 33 % of exergetic efficiency, within 95 % of confidence level. The patterns of the emissions revealed the important effect of the increased ignition delay time of the straight vegetable oil. Therefore, although preheating was used to adjust the fuel properties to provide similar spray regimes, the blending with diesel oil had an important effect in reducing the ignition delay time.

Keywords Biofuels · Straight soybean oil · Compression ignition engines · Thermodynamic analysis

Abbreviations

ANOVA	Analysis of variance
BSFC	Brake specific fuel consumption
LHV	Low heating value
SVO	Straight vegetable oil

List of symbols

c	Carbon atoms in the fuel molecule
C	Carbon
\bar{c}_p	Specific heat of fuel [kJ/(kmol K)]
\bar{e}	Specific flow exergy (kJ/kmol)
\dot{E}	Exergy rate (kW)
h	Hydrogen atoms in the fuel molecule
H	Hydrogen
\bar{h}	Specific enthalpy (kJ/kmol)
\dot{m}	Mass flow rate (kg/s)
N	Nitrogen
\dot{n}	Molar flow rate (kmol/s)
o	Oxygen atoms in the fuel molecule
O	Oxygen
P	Pressure (Pa)
\dot{Q}	Heat transfer rate (kW)
\bar{R}	Universal gas constant [kJ/(kmol K)]
S	Sulfur
\bar{s}	Specific entropy [kJ/(kmol K)]
\dot{S}	Entropy production rate (kW/K)
T	Temperature (°C)
y	Mole fraction
\dot{W}	Power (kW)

Greek symbols

η	Energetic efficiency
ε	Exergetic efficiency

Technical Editor: Luis Fernando Figueira da Silva.

N. A. Nieto Garzón (✉) · A. A. M. Oliveira ·
R. M. Hartmann · E. Bazzo
Laboratory of Combustion and Thermal Systems Engineering
(LabCET), Federal University of Santa Catarina, Florianópolis,
SC CEP: 88040-900, Brazil
e-mail: nury@labcet.ufsc.br

Subscripts

a	Air
D	Destruction
f	Fuel
g	Gas
<i>i</i>	<i>i</i> th Mixture component
in	Input
m	Engine surface temperature
o	Reference state
out	Output
s	Stoichiometric

Superscripts

ch	Chemical exergy
e	Reference environment
ph	Physical exergy

1 Introduction

Energy security, economics and environmental impacts associated with the use of fossil fuels have renewed the interest in the use of biofuels. In recent decades, several studies addressed the use of vegetable oils and biodiesel in compression ignition engines, both for transport and for stationary energy generation. In Brazil, some studies have been conducted in regard to the use of vegetable oils, especially of the crude palm oil, for electric power generation in remote regions [1–6]. The differences in the thermo-physical properties of vegetable oils when compared to diesel oil, especially density, viscosity, ignition delay and propensity for the formation of soot and combustion chamber deposits, are the main drawbacks addressed by the researchers. Other concerns are related to conservation and degradation during storage, but these are not addressed here.

Vegetable oils are mostly polyunsaturated triglycerides. They have a smaller ratio of hydrogen to carbon atoms and, therefore, a smaller lower heating value (LHV) when compared with diesel oil. The large molecules of vegetable oils and their unsaturated carbon chain lead to high viscosity and low volatility [6, 7]. Viscosity and density are key properties in the fuel atomization in direct injection systems. The high viscosity of vegetable oils causes poor atomization, characterized by large average droplet size, small jet angle, and high penetration length. As a result, fuel vaporization and mixing is prevented, leading to poor combustion, resulting in high emissions and loss of engine power [6, 8]. The transformation of vegetable oils in biodiesel through the transesterification reaction minimizes these disadvantages [7]. However, as a by-product, glycerol is produced, which requires purification before it can be used in other industrial applications.

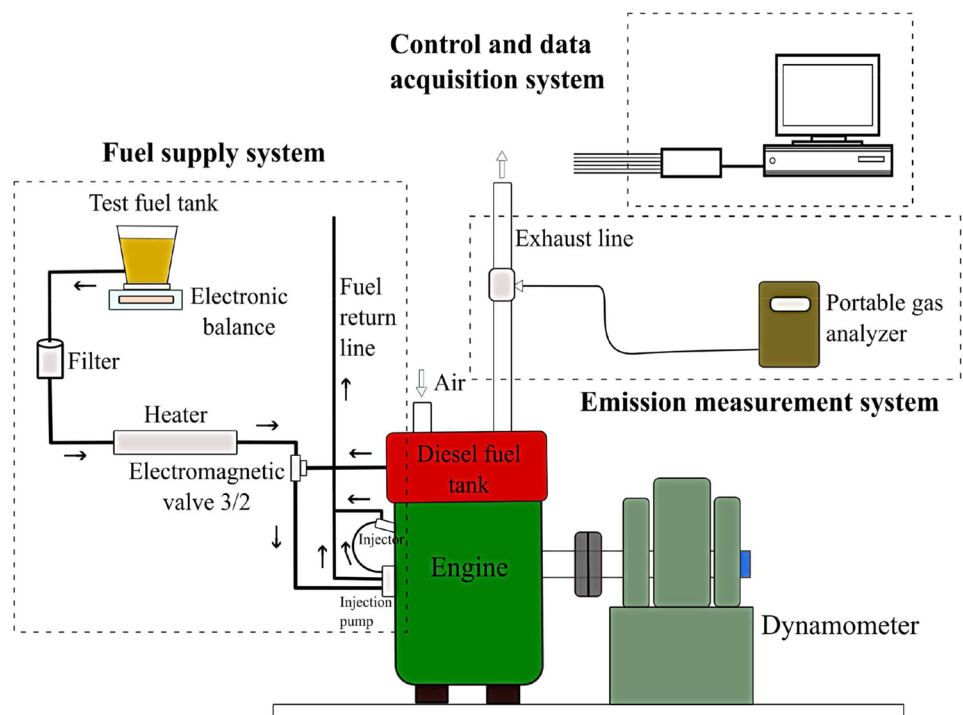
The direct combustion of glycerol has been addressed, but with relative success. The feasibility of using raw vegetable oils directly in compression ignition engines allows for a more direct use, with a minimum of processing operations [9].

Blending with diesel oil has been studied as a simple way of reducing the viscosity of vegetable oils. Tests with vegetable oils obtained from rapeseed, palm, sunflower and soybean are found in the literature [11–13]. These tests showed a reduction in the power and increase in the specific fuel consumption when compared to neat diesel fuel. The blends with over 20 % vegetable oil content presented poor combustion. Heating the fuel before injection is another way of reducing the viscosity of vegetable oils. Preheating is effective and allows the engine to operate with 100 % vegetable oil for brief periods without modifying the engine [13, 14]. Increasing the injection pressure to improve atomization has also been studied, in pressures from 180 to 240 bar [16, 17]. In this small pressure range, there was a marginal increase in the thermal efficiency [17] but a significant reduction in the emissions of HC and soot as the injection pressure was increased.

Very few studies have addressed the thermodynamic analysis of the use of straight vegetable oils (SVO) in internal combustion engines. The energetic and exergetic analysis of internal combustion engines provide information on the energy and potential exergy flows, which is essential in the development of integrated energy systems such as cogeneration. Studies have focused either the engine cylinder [7, 17–19, 21–23] or the entire engine [24–26] as the control volume for analysis. Statistical techniques are useful to analyze the consistency of the results of thermodynamic studies. Tat [27] used Student's *t* test to compare the exergetic efficiency of four types of biodiesel with different cetane numbers. Nevertheless, there are few thermodynamic studies in the literature where statistical techniques have been applied to assess the statistical significance of the results regarding the experimental uncertainties, especially involving the use of SVO as fuels.

In this study, an experimental and thermodynamic analysis on the performance of a single-cylinder, four stroke, naturally aspirated, direct injection, compression ignition engine is presented. The engine was operated with 100 % raw soybean oil and a blend of diesel and soybean oils in the volumetric proportion of 1:1, using the same injection system. Preheating was used to reduce the fuel viscosity before the injection pump. The results were compared with those obtained for diesel oil using two statistical techniques: analysis of variance (ANOVA) and Dunnett's test. Dunnett's test is appropriate for the comparison with a standard parameter, which in this case was the performance with diesel oil.

Fig. 1 Schematic overview of the dynamometric bench



1.1 Experiment

1.1.1 Engine and experimental setup

Performance and emissions of a 14.7 kW, naturally aspired, mechanically injected and controlled, direct injection, single-cylinder, compression ignition engine (Yanmar, model YT22) connected to an electromagnetic steady-state dynamometer (Schenk, W70 model) were measured as a function of the engine speed. A schematic of the engine mounted on the dynamometric bench is presented in Fig. 1. Table 1 presents the engine’s main characteristics.

The engine’s mechanical speed control system uses a flyball governor for fuel control and as speed limiter. The flyball controller is in contact with a spindle that acts in the injection pump, controlling the pump volumetric displacement. When the engine speed increases, the governor decreases the volumetric displacement, and vice versa, in an attempt to keep a constant speed. When the speed exceeds 2,000 rpm, the volumetric displacement is reduced to a minimum. For the tests reported here, the engine’s controller was adjusted to full load.

The experimental setup was equipped with fuel supply, emission measurement, control, and data acquisition systems. The intake air had the temperature and humidity controlled to 22 °C and 60 %. An electric heater comprised of an aluminum tube (12.7 mm diameter), electrical resistance of 108 Ω and ceramic insulation was designed to pre-heat the SVO and the blend before injection. Type-J

Table 1 Basic characteristics of the engine as provided by the manufacturer

Manufacturer/model	Yanmar/YT22
Main characteristics	
Bore (mm)	115
Stroke (mm)	115
Compression ratio	17.3
Displacement volume (cm ³)	1,194
Nominal performance	
Speed (rpm)	2,000
Power (kW)	14.7
BSFC [g (kWh) ⁻¹]	238
Air mass flow (kg/s)	0.021
Injection pressure (bar)	200
Injection timing (BTDC)	18

thermocouples were installed in the engine cooling water inlet and outlet, in the exhaust and the intake manifolds. Resistive sensors (Thermistor, NTC) were installed at the heater outlet and the injection pump inlet. A three-way electromagnetic valve was installed to switch the engine fuel. The fuel consumption was measured using a Shimadzu electronic balance, model 8200S UX, with serial communication. The engine torque was measured with an Hbm Wagezelle extensometer type-load cell installed on the dynamometer lever. The speed was measured with an incremental encoder 60 pulses/second coupled to the

Table 2 Physical–chemical properties of the fuels used

Property	100S	50S/50D	100D
C (wt%) ^a	76.91	80.63	84.6 ^b
H (wt%) ^a	11.40	13.32	15.4 ^b
N (wt%) ^a	2.03	1.03	–
O (wt%)	9.66	5.03	–
S (mg/kg) ^a	1.24	864	1,800 ^c
LHV (kJ/kg) ^a	36,333	39,191	42,287 ^d
HHV (kJ/kg) ^a	38,791	41,776	45,008 ^d
Density (kg/m ³) ^e	880 (at 85 °C)	856 (at 65 °C)	848 (at 25 °C)
Volumetric heating value (MJ/m ³)	31,940.3 (at 85 °C)	33,559.3 (at 65 °C)	35,732.5 (at 25 °C)
Air/fuel ratio (kga/kgf) ^s	12.3	13.6	14.9
Flash point (°C) ^f	292	–	38
Rams bottom carbon residue (wt%) ^f	0.482	–	0.25
Oxidation stability (h) ^a	4.64	–	–
Cetane number	37.9 [30]	–	47 [30, 32]
	38.1 [31]		50 [33]
	38 [32]		48 [34]
	36–38 [33]		

^a Proprieties measured by National Institute of Technology, Brazil

^b Taken as C₁₂H₂₆

^c Regulated by National Agency of Petroleum, Natural Gas, and Biofuels [28]

^d From Ministry of Mines and Energy [29]

^e Measured at Laboratory of Combustion and Thermal Systems Engineering, Federal University of Santa Catarina, Brazil

^f Proprieties measured by Technology Institute of Paraná, Brazil

dynamometer shaft. The concentrations of the exhaust gases (CO, CO₂ and NO_x) were measured with a Testo portable gas analyzer, model 350-XL, whose probe was installed in the exhaust pipe. The tests were controlled by an electronic control system coupled to the LabVIEW 7.1 software.

1.1.2 Fuels

The fuels tested were straight soybean oil, commercial Brazilian diesel oil (known as diesel S1800) and a blend of soybean and diesel oils in a volumetric proportion of 1:1. Commercial Brazilian diesel oil has a volumetric addition of 5 % of biodiesel in accordance with national regulations [28]. Soybean oil was chosen due to its high production and availability in Brazil. It suffered no refining or transesterification; only filtering. The fuels were labeled as: 100S—raw soybean oil, 100D—diesel fuel and 50S/50D—blend of soybean and diesel oils.

The main physical and chemical properties of the soybean oil, diesel fuel and the blend are presented in Table 2. It can be observed that the soybean oil has the lowest LHV, about 14 % smaller when compared to diesel oil. This is associated with the smaller content of carbon and hydrogen and the nature of the bonds in the molecular structure. Figure 2 presents the density and the dynamic viscosity of each fuel measured at different temperatures. The viscosity was measured using a Thermo Electron viscometer model HAAKE VT550 while the density was measured using Archimedes' principle. The density changes with temperature in a similar way for the three fuels analyzed. At 85 °C, soybean oil has a density 4.4 % smaller than at room

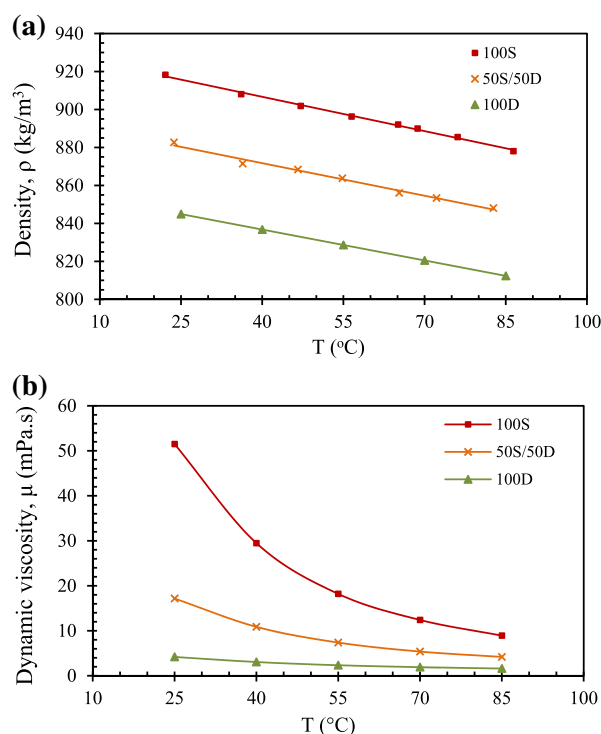


Fig. 2 a Density and b dynamic viscosity of the fuels used measured as a function of temperature

temperature. The viscosity reduces with temperature and approximates that of diesel oil at 25 °C. The viscosity of soybean oil at 85 °C remains approximately 113 % higher than the viscosity of diesel oil at 25 °C. The measurement of viscosity allowed estimating the temperature required to

bring the viscosity of the biofuel close to that of diesel oil at room temperature.

1.1.3 Experimental procedure

The biofuels were heated before the injection pump in an attempt to work under the same spray regime for all the fuels tested (fuel injector Reynolds number around 6,000 and Ohnesorge number around 0.1, within the atomization regime [35, 36]). The selected heating temperatures were 85 °C for the 100S and 65 °C for the 50S/50D oils. The electrical resistance and the supplied voltage were measured during the process of fuel heating. The 100D oil was fed to the injection pump at room temperature. The same injector (original, from the manufacturer) was used in all tests. The tests were all performed at the maximum volumetric flow rate of the injection pump.

In each test, the engine started with zero load and was allowed to operate with diesel oil until the cooling water temperature reached 70 °C. The fuel was then switched to the test fuel. After reaching stable operation with the new fuel, the brake was progressively applied, allowing for a sequence of steady-state measurements in the interval from 2,200 to 1,400 rpm. At each load, the steady-state operation was verified by the stabilization of the emissions. Measurements of torque, speed, fuel consumption, and concentrations of CO, CO₂ and NO_x in the exhaust gases were then recorded at intervals of 10 s resulting in fifteen readings for each load condition. The tests with each fuel were performed three times to verify repeatability. In the case of the 100S and 50S/50D oils, before turning the engine off at the end of the test, the fuel was switched back to diesel oil allowing the engine to operate for a period of 20 min. The aim of this was to dissolve deposits in the fuel lines to prevent clogging of the fuel supply system.

The measurements were statistically analyzed applying ANOVA and Dunnett’s tests. The statistical analysis was performed considering a confidence interval of 95 % using the software Minitab 14. Table 3 presents the expanded measurement uncertainties. The uncertainty of the reported measurements was estimated considering the uncertainty of the instruments used for the different measurements and the statistical uncertainty related to the number of experiments.

The air mass flow rate admitted to the engine was not directly measured, but back calculated from the carbon and oxygen balance, based on the recorded emissions of CO₂ in the exhaust gases and on the assumption of a complete combustion with excess air. It is observed that neglecting the CO concentration results in an error smaller than 0.5 %. Therefore, the presence of CO in the exhaust gases was not considered in the thermodynamic analysis that follows.

Table 3 Expanded uncertainty of each measurement

Measurements	Expanded uncertainty (%)
Engine speed	±2.5
Break torque	±2.8
Power	±2
Fuel mass rate	±5
Specific fuel consumption	±4
CO	±9
CO ₂	±5
NO _x	±8
Exhaust gas temperature	±0.8

Expanded uncertainty as a percentage of the mean value for a probability of 95 %

1.2 Thermodynamic analysis

Figure 3 depicts the control volume selected for the energetic and exergetic analyses. The following assumptions were made: (1) the reference environment remains at $T_0 = 25\text{ °C}$ and $p_0 = 101,325\text{ Pa}$; (2) the control volume, an open system, is under steady-state conditions; (3) kinetic and potential energy effects are negligible; (4) the combustion air and exhaust gases are ideal gas mixtures; (5) the fuel suffers complete reaction to saturated combustion products; and (6) the engine surface temperature corresponds to the average cooling water temperature.

The energy balance for the control volume on the basis of 1 kmol of fuel is written as

$$\frac{\dot{Q}_{out}}{\dot{n}_f} - \frac{\dot{W}_{out}}{\dot{n}_f} = \bar{h}_g - \bar{h}_f - \bar{h}_a \tag{1}$$

where \dot{Q}_{out} is the heat transfer rate to the environment, \dot{W}_{out} is the brake engine power, \dot{n}_f is the molar flow rate of the fuel and \bar{h}_g , \bar{h}_f and \bar{h}_a are the enthalpies of the exhaust gases, fuel and air, respectively, expressed per kmol of fuel.

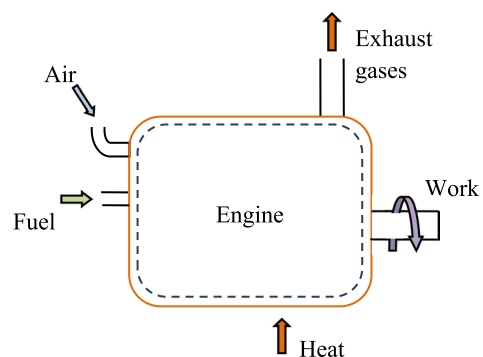


Fig. 3 Control volume of the thermodynamics system of the diesel engine

Table 4 Gaseous reference species at 298.15 K and 101.325 kPa [37]

Chemical species	Mole fraction in dry air
N ₂	0.780 30
O ₂	0.209 90
CO ₂	0.000 35
Ar	0.009 33

The absolute enthalpy of the fuel is obtained from the enthalpy of formation and the variation of sensible enthalpy, given as

$$\bar{h}_f = \bar{h}_{f,o} + \bar{c}_p(T_f - T_o) \tag{2}$$

where \bar{c}_p is the average molar specific heat of the fuel, T_f is the fuel temperature and $\bar{h}_{f,o}$ is the enthalpy of formation of the fuel at the reference standard state. The enthalpy of formation of the fuel is determined from the measured fuel lower heating value (LHV) assuming complete combustion with air to saturated combustion products:

The energy lost in the exhaust gases is calculated as

$$\dot{Q}_g = \dot{m}_f \text{LHV} + \dot{W}_{in} - \dot{W}_{out} - \dot{Q}_{out} \tag{3}$$

where \dot{Q}_g is the rate of energy lost in the exhaust gases, \dot{m}_f is the mass flow rate of the fuel and \dot{W}_{in} is the electric power supplied to heat the fuel.

The energy efficiency is defined as the ratio of the brake engine power to the fuel energy input rate,

$$\eta = \frac{\dot{W}_{out}}{\dot{m}_f \text{LHV} + \dot{W}_{in}} \tag{4}$$

The exergy balance for the control volume on the basis of 1 kmol of fuel is written as

$$\dot{n}_f(\bar{e}_f + \bar{e}_a - \bar{e}_g) + \dot{W}_{in} - \dot{Q}_{out} \left(1 - \frac{T_o}{T_m}\right) - \dot{W}_{out} = \dot{E}_D \tag{5}$$

where \bar{e}_f , \bar{e}_a , and \bar{e}_g are the specific flow exergies of the fuel, combustion air and exhaust gas, respectively, \dot{W}_{in} is the system power input related to the electric power of the preheating, \dot{E}_D is the exergy destruction rate, and T_m is the engine surface temperature.

Since the fuel enters the system in a condition relatively close to the reference state, the specific physical exergy of the fuel was disregarded and only the specific chemical exergy was considered, which was calculated according to Szargut et al. [37] as

$$\bar{e}_f^{ch} = \text{LHV} \left(1.0374 + 0.01594 \frac{h}{c} + 0.0567 \frac{o}{c}\right) \tag{6}$$

The specific flow exergy of the combustion air was also neglected since the air enters the system in a state relatively close to the reference state. The specific exergy of exhaust gases is formed by the specific physical exergy and the specific chemical exergy of the gas mixture. The specific physical exergy of the gas mixture is calculated as

$$\bar{e}_g^{ph} = \sum_{i=1}^N n_i \left\{ \bar{h}_{i,(T)} - \bar{h}_{i,o} - T_o \left[\bar{s}_{i,(T,p_o)} - \bar{s}_{i,o} - \bar{R} \ln \frac{p_i}{p_o} \right] \right\} \tag{7}$$

where \bar{e}_g^{ph} is specific physical exergy of the exhaust gases, $\bar{h}_{i,(T)}$ and $\bar{h}_{i,o}$ are the enthalpies of the i th component at temperatures T and T_o , respectively, $\bar{s}_{i,(T,p_o)}$ and $\bar{s}_{i,o}$ are the entropies of the i th component in (T,p_o) and (T_o,p_o) , respectively, \bar{R} is the universal gas constant, and p_i is the partial pressure of the i th component in the gas mixture. The specific chemical exergy of the gas mixture is calculated as

$$\bar{e}_g^{ch} = \bar{R} T_o \sum_{i=1}^N n_i \ln \left(\frac{y_i}{y_i^e} \right) \tag{8}$$

where \bar{e}_g^{ch} is the specific chemical exergy of exhaust gases, y_i is the mole fraction of the i th component in the exhaust gases for (T,p) and y_i^e is the mole fraction of the i th component in the reference environment. The reference environment according to Szargut et al. [37] is presented in Table 4. As stated above, the exhaust gases are considered as an ideal gas mixture of CO₂, H₂O, N₂ and O₂.

The exergy destruction is obtained from Eq. (5) and the entropy production rate \dot{S} from the following relation

$$\dot{E}_D = T_o \dot{S} \tag{9}$$

The exergy efficiency is defined as the ratio between the net exergy work rate and the rate of exergy input into the system,

$$\varepsilon = \frac{\dot{W}_{out}}{\dot{E}_{in}} \tag{10}$$

where \dot{E}_{in} is the rate of exergy input estimated as the sum of the fuel exergy and the power input to the system, according to Eq. (11),

$$\dot{E}_{in} = \dot{n}_f \bar{e}_f + \dot{W}_{in} \tag{11}$$

The values measured for the engine performance parameters, air admission temperature and exhaust gas temperature, as well as the chemical composition of the fuels, were used as inputs to the thermodynamic analysis. The analysis was performed at 1,800 rpm, which is the nominal speed required by a 4 poles, 60 Hz electrical generator. The calculations were performed using the software engineering equation solver (EES).

2 Results and discussion

2.1 Engine performance

Figure 4 presents the mean values of brake torque and power as a function of engine speed for the three different fuels tested. The respective expanded uncertainty of the measurements is also shown as uncertainty bars. The fixed purely mechanical engine control results in a strong variation of engine speed with the applied brake torque. The highest and lowest powers were obtained with the 100D oil and the 100S oil, respectively. The 50S/50D blend presented intermediate values of torque and power, a behavior proportional to the ratio of the values of LHV. The performance above 2,000 rpm falls abruptly. This high speed regime is mechanically limited by the governor. Therefore, in the figures that follow, all measurements taken above 2,000 rpm, marked by the dashed line in Fig. 4 are excluded. The electric power supplied to heat the fuel was calculated as 0.224 kW for 100S oil and 0.180 kW for 50S/50D blend.

At 1,800 rpm, the mean power values for the 100S oil, the 50S/50D blend and the 100D oil were 11.17, 11.70 and 12.9 kW, respectively, which followed the difference in LHV. The ANOVA test identified a significant difference

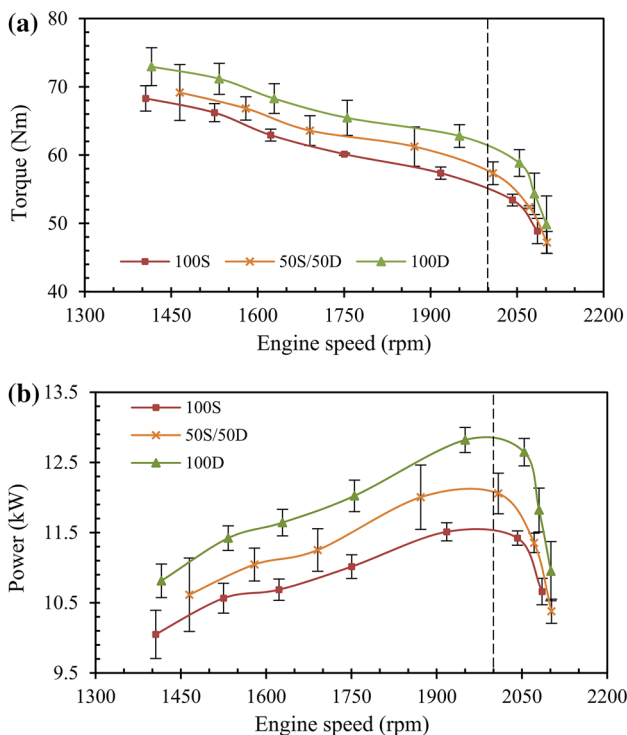


Fig. 4 **a** Brake torque and **b** brake power as a function of the engine speed for the operation with the three different fuels (injection temperatures, respectively, of 25, 65 and 85 °C for 100D, 50D/50S and 100S)

($p = 0.002$) between the mean power of the fuels tested. The Dunnett’s test found statistically significant differences for the comparison of the 100S and the 100D oils ($p < 0.05$), but not for the comparison between the 50S/50D and the 100D ($p > 0.05$). In conclusion, the engine power using 100S oil at 1,800 rpm was 7.6 % lower when compared with the corresponding value for 100D oil.

Figure 5a presents the fuel mass injected per cycle for the different fuels, as a function of engine speed. The pump volumetric displacement increases when the engine speed decreases, since the flyball governor acts in the direction of trying to keep a constant speed. Therefore, for all fuels, the mass injected per cycle is larger at lower speeds. Considering the differences among the fuels at constant speed, i.e., constant volumetric displacement, the mass injected per cycle is proportional to the fuel density. Therefore, at constant speed, the denser oil, the 100S oil, results in higher mass pumped per cycle. Figure 5b presents the brake-specific fuel consumption (BSFC). The relative difference among the fuels scales with the volumetric heating values (Table 1). At 1,800 rpm, the specific fuel consumptions are 272 g/kWh (100S), 257 g/kWh (50S/50D), and 242 g/kWh (100D), a 12 % increase for the 100S oil and a 6 % increase for the 50S/50D blend. These were statistically significant according both to the ANOVA and the Dunnett’s tests ($p < 0.05$). Figure 5c presents the exhaust gas temperature. Higher exhaust temperatures were observed with the 100D oil. Since the valve scheduling is the same for all fuels, this behavior agrees with the relation among the heating values, indicating higher average engine temperature for the 100D. For the same fuel, especially evidenced by the 100D, when the speed increases, the exhaust temperature first decreases and then increases. At lower speeds, the increase in exhaust temperature is a result of the higher mass injected per cycle combined to the longer residence time of the fuel in the combustion chamber, allowing for a greater amount of fuel burned per cycle before blowdown. However, although more energy is evolved per cycle resulting in higher torque as evidenced in Fig. 4a, the combustion of the richer mixture also leads to higher CO emission, as shown in Fig. 6c. At higher speeds, the higher power results in higher engine temperature.

2.2 Emissions

Figure 6a presents the air/fuel ratio as a function of the engine speed. It is observed that the air/fuel ratio decreases with the reduction in the engine speed. This could be caused by a decrease in volumetric efficiency, decreasing the air intake per cycle, or by the increase in fuel mass per cycle presented in Fig. 5a. The reduction of air/fuel ratio shown in Fig. 6a is approximately 4 % at each 150 rpm reduction in speed. For the fuels tested, the variation of the air/fuel

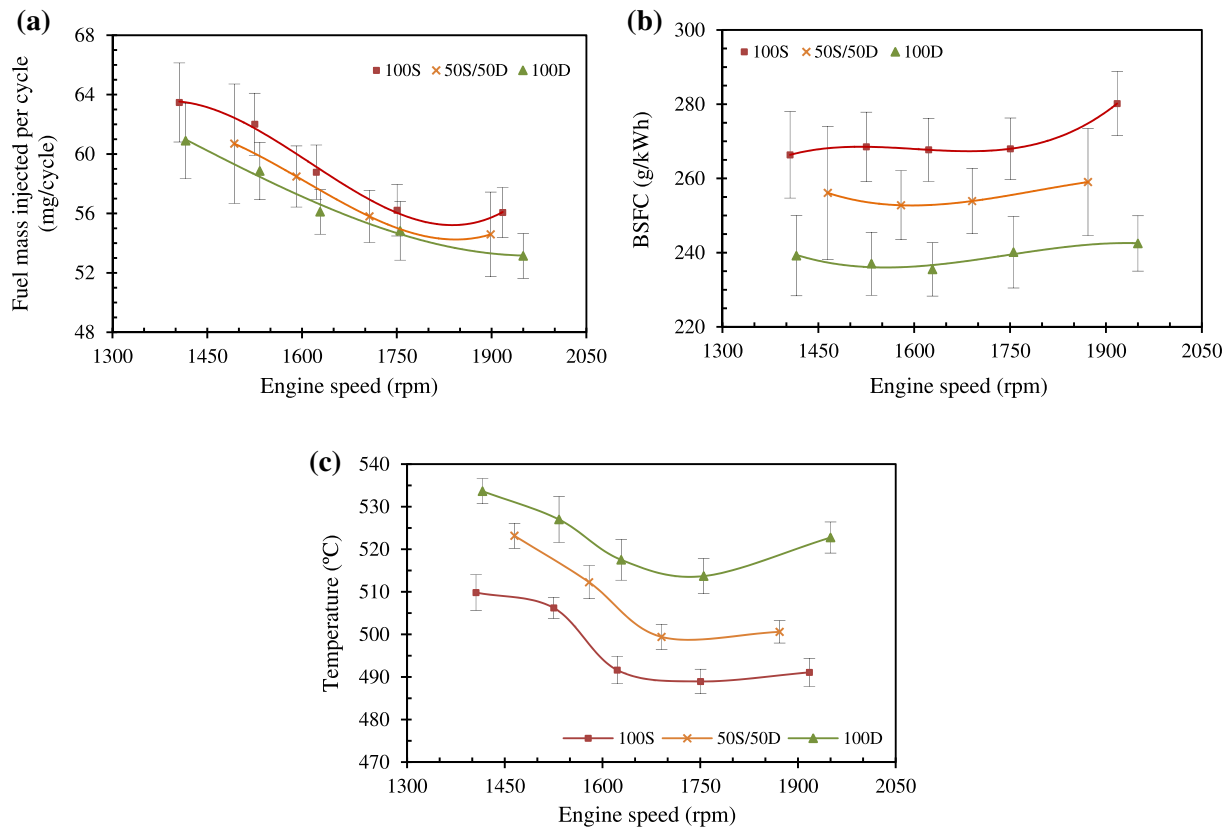


Fig. 5 **a** Fuel mass injected per cycle, **b** brake-specific fuel consumption and **c** exhaust gas temperature as a function of the engine speed for the operation with the three different fuels (injection temperatures, respectively, of 25, 65 and 85 °C for 100D, 50D/50S and 100S)

ratio caused by the reduction in the air intake accounts for approximately 0.5 % of this total, while the increase in fuel mass injected per cycle accounts for the remaining 3.5 %. Therefore, the behavior of the air–fuel ratio as a function of speed mostly reflects the action of the flyball governor in the fuel mass injected per cycle, as shown in Fig. 5a. Figure 6b presents the specific CO₂ emissions. The ratio among the fuels is consistent with the fuel mass injected per cycle. The specific emissions, within the uncertainties, remain constant with the engine speed. Figure 6c presents the specific CO emissions. An increase in the CO emissions at low engine speed is observed for all fuels as a consequence of the greater mass of fuel injected per cycle, as shown in Fig. 5a, leading to the smaller air fuel ratio shown in Fig. 6a. Even though there is a larger residence time, leading to a higher production of work, the fuel burned late results in a higher production of CO. The 100S fuel, as a result of lower engine temperature and longer ignition delay time, emits the highest amount of CO. An addition of diesel oil to the soybean oil, decreases the ignition delay, causing a decrease in the emission of CO. As observed in Fig. 6c, the 50S/50D fuel emits basically the same specific amount of CO as the 100D fuel, showing the important

effect of the ignition delay time. Figure 6d presents the specific NO_x emission. Due to the lower LHV and longer ignition delay, the S100 fuel results in the lowest temperature in the combustion chamber, resulting in the lowest production of NO_x by the thermal (Zeldovich) mechanism [38]. The presence of fuel bound N in the 100S contributes to approximate the NO_x emission of the 50S/50D to that of the 100D fuel. However, the main effect is again the ignition delay. A longer ignition delay leads to lower pressures and temperatures in the combustion chamber, decreasing the thermal production of NO_x. The improvement of ignition delay, caused by the addition of diesel fuel, makes the NO_x emission of the 50S/50D to be the same as the 100D. This trend remains consistent with the behavior exhibited by the exhaust gas temperature. The longer ignition delay extends the post-combustion to the opening of the exhaust valve, an effect that causes an increase in the temperature of the exhaust gases [1, 39]. However, the LHV effect prevails in the exhaust gas temperature, resulting in the behavior shown in Fig. 5c. The ignition delay has physical, such as atomization, evaporation and mixing, and chemical causes, related to the thermal ignition in the premixed region. Both are affected by the fuel composition, spray,

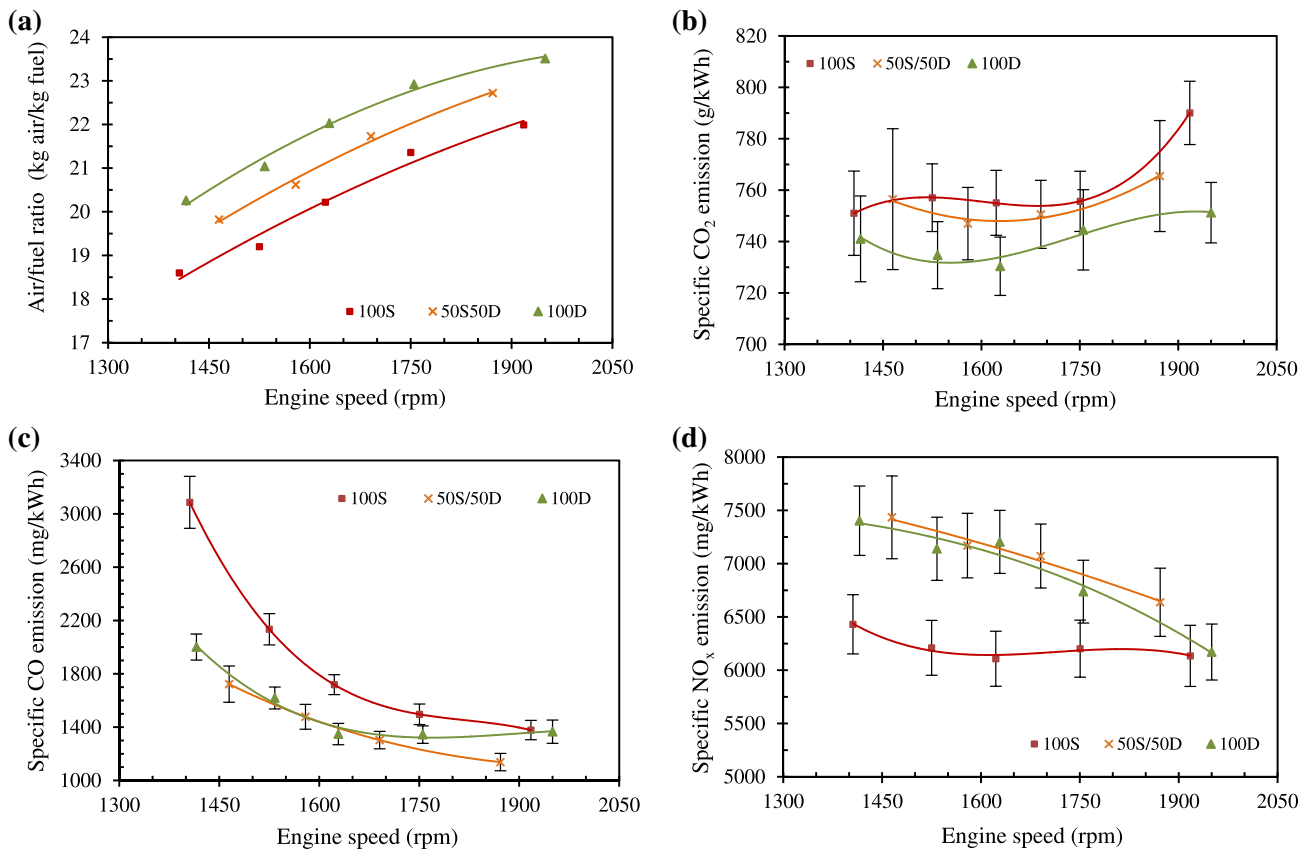


Fig. 6 a Air/Fuel ratio, b specific CO₂ emission, c specific CO emission, and d specific NO_x emission as a function of engine speed

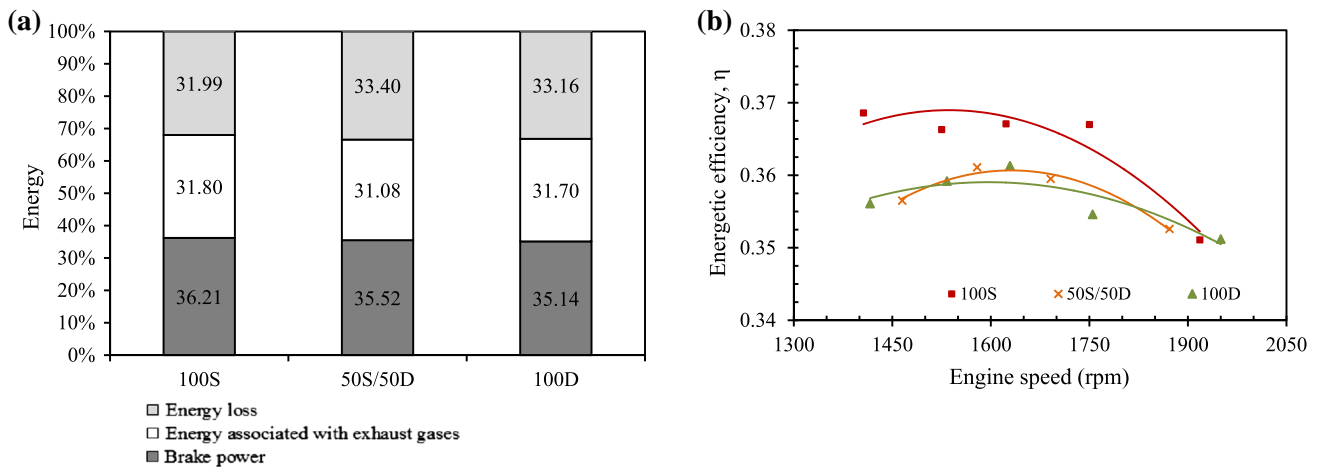


Fig. 7 a Energy balance at 1,800 rpm and b fuel conversion efficiency (1st Law efficiency) versus engine speed. In part a, from bottom to top, are the engine power, the energy associated with the exhaust gases, and the heat transfer to the ambient

and engine operating parameters. The increase in injection pressure [10, 11] and an injection advance when operating with SVO [39] (because to its lower compressibility), may reduce the effects of ignition delay.

2.3 Energy analysis

Figure 7a presents the overall engine energy balance at 1,800 rpm. The 100S presents the maximum energy

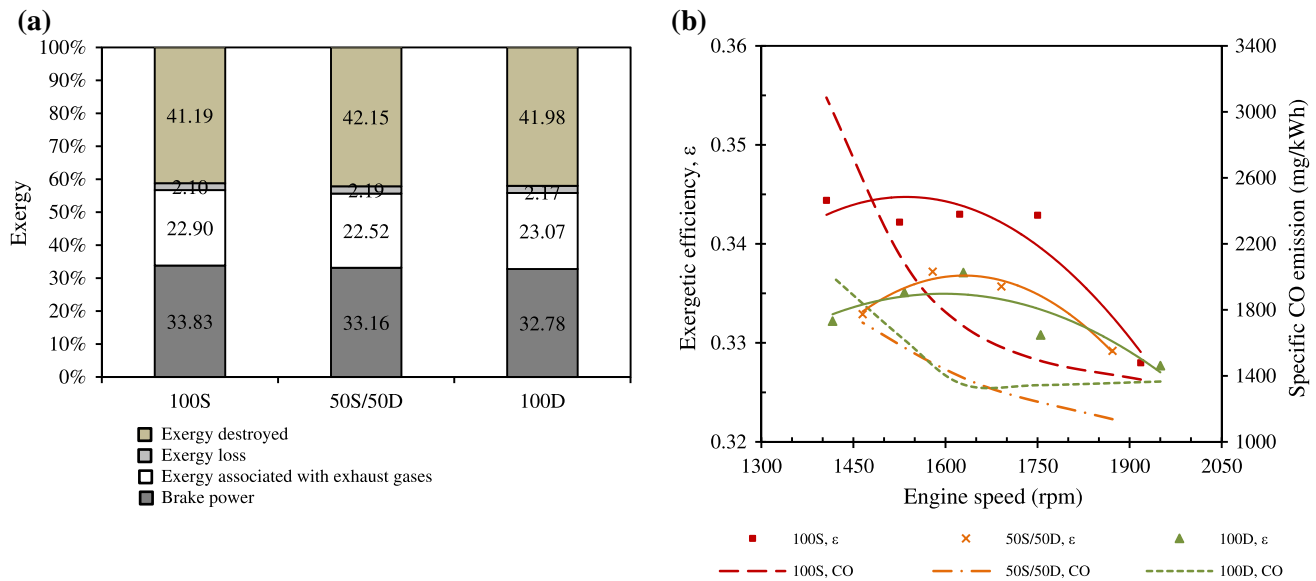


Fig. 8 **a** Exergy balance at 1,800 rpm and **b** exergetic efficiency (2nd Law efficiency) versus engine speed. In part **a**, from bottom to top, are the exergy related to the engine power, the exergy associated to the exhaust gases, the exergy loss to the ambient and the exergy destroyed

efficiency of 36.2 %, followed by the 50S/50D with 35.5 % and the 100D with 35.1 %. The difference is only marginal and is mainly caused by the increased engine temperature when operating with neat diesel. The statistical analysis with ANOVA did not show a significant difference ($p = 0.088$). Figure 7b presents the energetic efficiency (fuel conversion efficiency) as a function of the engine speed. The curves present a maximum at 1,600 rpm and tend to overlap at higher speeds. The behavior of the thermal efficiency in these tests is the result of the combined effects of the fuel injected per cycle and the residence time. At higher speeds, the shorter residence time for combustion leads to a release of combustion products before their energy is converted to torque. This effect, combined with the leaner mixture, results in the decrease of the torque produced, as evidenced in Fig. 4a. This early release of burned gases is also consistent with the increase in exhaust gas temperature, as shown in Fig. 5c, and the lower production of NO_x , as shown in Fig. 6d, since NO_x requires longer residence time to be produced. As a consequence, the thermal efficiency decreases at higher speeds. At lower speeds, there is much excess of fuel, as noted above. This excess fuel produces a higher torque, but with the penalty of a larger fuel consumption. This is also consistent with the higher production of CO at lower speeds, due to the partial combustion of the fuel injected later. The 100S follows basically the same trend. At lower speeds, the longer residence time allows for the more complete combustion of the 100S fuel (also observed in Balafoutis et al. [11]), which is somewhat offset by the lower temperatures achieved

at lower power. The most interesting aspect is the higher thermal efficiency for the 100S fuel when compared to the 100D. Considering the lower volumetric heating value, the increased combustion obtained at longer residence time provides the extra efficiency. The 100S fuel also presents oxygen in its composition, which may increase the extent of combustion. Additionally, the content of unsaturated fatty acids favors the air/fuel mixture because the oxygen of the air reacts with unsaturated bonds of the vegetable oil [11]. For the soybean oil, 85 % of its fatty acids have double or unsaturated bonds.

2.4 Exergy analysis

Figure 8a presents the exergy balance at 1,800 rpm. From the ANOVA test, there was no significant statistical difference between the exergetic efficiencies of the three fuels ($p = 0.075$), the exergy destroyed ($p = 0.308$), or the exergy of the exhaust gases ($p = 0.574$). The lower exergy destruction for the 100S is also related to the longer ignition delay time. An increase in the ignition delay results in smaller variation in the temperature and pressure in the combustion chamber, which results in lower exergy destruction [22, 27]. Figure 8b compares the exergetic efficiency to the CO emission as a function of engine speed. The best performance must combine high efficiency to low emission. This occurs in the range between 1,600 rpm and 1,700 rpm for the three fuels. This range corresponds to medium loads of 10.7, 11.2 and 11.7 kW for the 100S, 50S/50D and 100D oils, respectively.

3 Conclusions

The performance of a single-cylinder, naturally aspirated, mechanically pumped and controlled, direct injection, compression ignition engine, operating with three fuels, was assessed. The fuels were diesel oil (100D), straight soybean oil (100S) and a blend of 50 % (v/v) diesel oil and soybean oil (50D/50S). The injection system and engine parameters were kept the same for all the fuels tested. To reproduce a similar spray regime for all fuels tested, the 100D was supplied at 25 °C, the 50D/50S at 65 °C and the 100 S at 85 °C. Steady-state measurements of brake torque, fuel consumption, exhaust gas temperature and gas pollutant emissions, combined with a thermodynamic analysis, allowed evaluating the engine performance operating with each fuel at speeds from 1,400 rpm to 2,000 rpm. Two statistical techniques, analysis of variance (ANOVA) and Dunnett's test were used to compare the measurements for the biofuels with those of the diesel oil, considered as the standard fuel.

The results indicated a higher brake power for the operation with diesel oil, but, similar thermal efficiency for the operation with all fuels tested, over the entire range of engine speed. The differences observed for the behavior of the engine operating with the different fuels are mainly determined by the trends in lower heating value, density, and ignition delay for the fuels tested. The variations observed with engine speed are mainly determined by the trends of mass of fuel injected per cycle and residence time.

In regards to the behavior of the operation with the different fuels, the results of engine torque were consistent with the trends in heating values for the fuels tested. Diesel oil presents a higher LHV, resulting in higher production of torque, higher exhaust gas temperature, and higher production of NO_x for the entire range of engine speed. The soybean oil presents a higher ignition delay, mainly as a result of the poorer atomization. The higher density results in higher mass of fuel injected per cycle, but still not enough to compensate for the lower LHV. Therefore, the effects of larger density and longer ignition delay combine to result in higher production of CO, smaller exhaust gas temperature and smaller production of NO_x in the entire range of engine speed. It is still not possible to pinpoint how these effects combine to give the soybean oil similar thermal efficiency than diesel oil.

Regarding the behavior with the engine speed, combined effects of the fuel mass injected per cycle and the residence time in the combustion chamber have a strong effect in the engine performance. At higher speeds, the shorter residence time for combustion leads to the exhaust of combustion products before their energy is completely converted to torque. This effect, combined with the smaller mass of fuel injected per cycle at higher speeds, results in the decrease of the torque produced. The early release of burned gases is also consistent with the increase in exhaust

gas temperature and the lower production of NO_x observed at higher speeds. As a consequence, the thermal efficiency decreases at higher speeds. At lower speeds, there is a higher mass of fuel injected per cycle, resulting in a richer mixture. This excess fuel produces a higher torque, accompanied by a higher exhaust gas temperature and a higher amount of NO_x, but with the penalty of a larger fuel consumption. This is also consistent with the higher production of CO at lower speeds, due to the partial combustion of the fuel injected later. This trend is more pronounced for the soybean oil due to the longer ignition delay time.

Considering the second law analysis, there was no statistically significant difference in the exergetic efficiency, exergy destroyed and exergy associated with the exhaust gases among the three fuels tested. The results revealed an exergetic efficiency of 33 %, exergy destruction rate of 42 % and exergy associated with exhaust gases of 23 %. For this engine in particular, the best performance range, that would combine high efficiency to low CO emission, occurs in the range between 1,600 rpm and 1,700 rpm for the three fuels. This range corresponds to medium loads of 10.7, 11.2 and 11.7 kW for the 100S, 50S/50D and 100D oils, respectively.

There is still a large room for improvement on the engine operation with SVO. Many physical, e.g., atomization, evaporation and mixing, and chemical, e.g., fuel composition and thermal ignition, effects determine the ignition delay and the development and intensity of the premixed and diffusion controlled combustion regimes of the SVO fuels. The increase in injection pressure and the use of an early injection when operating with SVO may reduce the physical effects on ignition delay. Chemically, the 100S fuel also presents oxygen in its composition, which may increase the extent of combustion. Additionally, the content of unsaturated fatty acids, 85 % (wt.) of the S100 are fatty acids, which have reactive double or unsaturated bonds, favors the air/fuel mixture. The possible gains in reduction of ignition delay remain to be better elucidated. Apparently, a combination of fuel preheating, blending with diesel oil, or other chemical species, increasing the injection pressure and advancing the injection timing may produce the best results. These effects remain to be elucidated further.

Acknowledgments The authors acknowledge Eletrosul Centrais Elétricas S.A. and the Brazilian Electricity Regulatory Agency—ANEEL for the financial support and CAPES for the scholarship for N. Nieto Garzón.

References

1. Almeida S, Belchior C, Nascimento M, Vieira L, Fleury G (2002) Performance of a diesel generator fuelled with palm oil. *Fuel* 81:2097–2102

2. Coelho ST, Silva OC, Velazquez SG, Monteiro MA, Silotto CG (2004) Energy from vegetable oil in diesel generators—Results of a test unit at amazon region. In: Proceedings of 3rd International Scientific Conference of Mechanical Engineering—Santa Clara, Cuba
3. Belchior C, Pimentel VB, Pereira PP (2006) The Research for the use of palm oil in diesel generators in the Amazon River. In: Proceedings of 2nd World Renewable Energy Congress Florence, Italy
4. Fonseca CM (2007) Substitution of the oil diesel by alternative fuels in the generation of electricity. Master thesis, Pontifical Catholic University of Rio de Janeiro (in Portuguese)
5. Duarte AR, Bezerra UH, de Lima ME, Duarte AM, da Rocha GN (2010) A proposal of electrical power supply to Brazilian Amazon remote communities. *Biomass Bioenerg* 34:1314–1320
6. Pereira RS, Tostes MEL, Nogueira MFM (2012) Evaluating indirect injection diesel engine performance fueled with palm oil. In: Proceedings of 14th Brazilian Congress on Thermal Science and Engineering—Rio de Janeiro, Brazil
7. Agarwal D, Kumar L, Agarwal AK (2008) Performance evaluation of a vegetable oil fuelled compression ignition engine. *Renew Energy* 33:1147–1156
8. Rakopoulos CD, Antonopoulos KA, Rakopoulos DC, Hountalas DT, Giakoumis EG (2006) Comparative performance and emissions study of a direct injection diesel engine using blends of diesel fuel with vegetable oils or bio-diesels of various origins. *Energy Convers Manage* 47:3272–3287
9. Franco Z, Nguyen QD (2011) Flow properties of vegetable oil-diesel fuel blends. *Fuel* 90:838–843
10. Hartmann RM, Garzón NN, Hartmann EM, Oliveira AAM, Bazzo E (2013) Vegetable oils of soybean, sunflower and tung as alternative fuels for compression ignition engines. *Int J Thermodyn* 16:87–96
11. Nwafor OM, Rice G (1996) Performance of rapeseed oil blends in a diesel engine. *Appl Energy* 54:345–354
12. Balafoutis A, Fountas S, Natsis A, Papadakis G (2011) Performance and emissions of sunflower, rapeseed, and cottonseed oils as fuels in an agricultural tractor engine. *ISNR Renew Energy* 531510:1–12
13. Chalalton V, Roy MM, Dutta A, Kumar S (2011) Jatropha oil production and an experimental investigation of its use as an alternative fuel in a DI diesel engine. *J Pet Technol Altern Fuels* 2:76–85
14. Nwafor OM (2004) Emission characteristics of diesel engine running on vegetable oil with elevated fuel inlet temperature. *Biomass Bioenerg* 27:507–511
15. Ozsezen A, Turkcan A, Canakci M (2009) Combustion analysis of preheated crude sunflower oil in an IDI diesel engine. *Biomass Bioenerg* 33:760–767
16. Venkanna BK, Wadawadagi SB, Reddy CV (2009) Effect of injection pressure on performance, emission and combustion characteristics of direct injection diesel engine running on blends of pongamia pinnata linn oil (honge oil) and diesel fuel. *Agric Eng Int* 11:1–17
17. SaradaSN Shailaja M, Raju AR, Radha KK (2010) Optimization of injection pressure for a compression ignition engine with cotton seed oil as an alternate fuel. *Int J Eng Sci Technol* 2:142–149
18. Van Gerpen JH, Shapiro HN (1990) Second-law analysis of diesel engine combustion. *J Eng Gas Turbines Power* 112:129–137
19. Rakopoulos CD (1993) Evaluation of a spark ignition engine cycle using first and second law analysis techniques. *Energy Convers Manage* 34:1299–1314
20. Alasfour FN (1997) Butanol—A single-cylinder engine study: availability analysis. *Appl Therm Eng* 17:537–549
21. Rakopoulos CD, Kyritsis DC (2001) Comparative second-law analysis of internal combustion engine operation for methane, methanol, and dodecane fuels. *Energy* 26:705–722
22. Benjumea P, Agudelo J, Agudelo A (2009) Effect of altitude and palm oil biodiesel fuelling on the performance and combustion characteristics of a HSDI diesel engine. *Fuel* 88:725–731
23. Bueno AV, Velasquez JA, Milanez LF (2011) Heat release and engine performance effects of soybean oil ethyl ester blending into diesel fuel. *Energy* 36:3907–3916
24. Canakci M, Hosoz M (2006) Energy and exergy analyses of a diesel engine fuelled with various biodiesels. *Energy Sour* 1:379–394
25. Gokalp B (2009) Biodiesel addition to standard diesel fuels and marine fuels used in a diesel engine: effects on emission characteristics and first and second-law efficiencies. *Energy Fuel* 23:1849–1857
26. Azoumah Y, Blin J, Daho T (2009) Exergy efficiency applied for the performance optimization of a direct injection compression ignition (CI) engine using biofuels. *Renew Energy* 34:1494–1500
27. Tat ME (2011) Cetane number effect on the energetic and exergetic efficiency of a diesel engine fuelled with biodiesel. *Fuel Process Technol* 92:1311–1321
28. National Agency of Petroleum, Natural gas, and biofuels (2011) Resolution ANP N° 65 of 9.12.2011—DOU 12.12.2011 (in Portuguese)
29. Ministry of Mines and Energy (2012) Brazilian energy balance 2012. EPE, Rio de Janeiro (in Portuguese)
30. Altin R, Çetinkaya S, Yücesu H (2001) The potential of using vegetable oil fuels as fuel for diesel engines. *Energy Convers Manage* 42:529–538
31. Demirbas A (2003) Biodiesel fuels from vegetable oils via catalytic and non-catalytic supercritical alcohol transesterifications and other methods: a survey. *Energy Convers Manage* 44:2093–2109
32. Ramadhas AS, Jayaraj S, Muraleedharan C (2004) Use of vegetable oils as I.C. engine fuels: a review. *Renew Energy* 29:727–742
33. Sidibé SS, Blin J, Vaitilingom G, Azoumah Y (2010) Use of crude filtered vegetable oil as a fuel in diesel engines state of the art: literature review. *Renew Sust Energy Rev* 14:2748–2759
34. Al-Dawody MF, Bhatti SK (2013) Optimization strategies to reduce the biodiesel NO_x effect in diesel engine with experimental verification. *Energy Convers Manage* 68:96–104
35. Reitz RD, Bracco FV (1982) Mechanism of atomization of a liquid jet. *Phys Fluids* 25:1730–1742
36. Martínez-Martínez S, Sanchez F, Bermudez V, Manuel J (2010) Liquid sprays characteristics in diesel engines. In: Siano D (ed) *Fuel Injection*. In Tech, <http://www.intechopen.com/books/fuel-injection/liquid-sprays-characteristics-in-diesel-engines>, pp 19–48
37. Szargut J, Morris D, Steward F (1988) Exergy analysis of thermal chemical and metallurgical processes. Springer, Berlin
38. Heywood JB (1988) Internal combustion engine fundamentals. McGraw-Hill, New York
39. Puhan S, Saravanan N, Nagarajan G, Vedaraman N (2010) Effect of biodiesel unsaturated fatty acid on combustion characteristics of a DI compression ignition engine. *Biomass Bioenerg* 34:1079–1088